An innovative methodology for quickly modeling the spatial-temporal evolution of domino accidents triggered by fire

Reference:
Chen Chao, Reniers Genserik, Zhang Laobing.- An innovative methodology for quickly modeling the spatial-temporal evolution of domino accidents triggered by fire
Journal of loss prevention in the process industries - ISSN 0950-4230 - 54(2018), p. 312-324
Full text (Publisher's DOI): https://doi.org/10.1016/J.JLP.2018.04.012
To cite this reference: https://hdl.handle.net/10067/1514120151162165141

An innovative methodology for quickly modeling the spatial-temporal evolution of domino accidents triggered by fire

Chao Chen[a], Genserik Reniers[a, b, c*], Laobing Zhang[a]

[a]Faculty of Technology, Policy and Management, Safety and Security Science Group (S3G), TU Delft, 2628 BX, Delft, The Netherlands
[b]Faculty of Applied Economics, Antwerp Research Group on Safety and Security (ARGoSS), University Antwerp, 2000, Antwerp, Belgium
[c]CEDON, KULeuven, Campus Brussels, 1000, Brussels, Belgium

*Corresponding author:
Email: g.l.l.m.e.reniers@tudelft.nl
Phone: +31 15 27 83749
Address: Jaffalaan 5, Delft 2628 BX, The Netherlands.

Abstract: Past accident analyses indicate that fire escalation is responsible for most of the domino effects that happened in the process industries. The evolution of domino accidents triggered by fire is different from domino accidents triggered by other primary scenarios, since the escalation caused by heat radiation is delayed with respect to the start of the fire. In this study, a methodology involving a Domino Evolution Graph (DEG) model and a Minimum Evolution Time (MET) algorithm is proposed to model the spatial-temporal evolution of domino accidents. Synergistic effects and parallel effects of the spatial evolution, as well as superimposed effects of the temporal evolution possibly occurring in complex domino evolution processes, are considered in this study. A case study demonstrates that the methodology is able to not only capture the spatial-temporal dimension but also to overcome the limitation of the "probit model" w.r.t only able to estimate the damage probability of the first level propagation. Besides, different from simulation or Bayesian approaches, our methodology can quickly provide evolution graphs (paths), the evolution time and the corresponding probability given a primary scenario. Therefore our approach can also be applied to domino risk assessment within an industrial park level and provide support for the allocation decision of safety and security resources.

Keywords: Domino effects; heat radiation; spatial-temporal evolution; Domino Evolution Graph; Minimum Evolution Time

1. Introduction

Safety and security are different in the nature of incidents: safety is unintentional whereas security is intentional (Hessami, 2004; Reniers and Pavlova, 2013). Regardless of the nature of incidents, they may become a primary accident in a chain of accidents, a phenomenon which is well known as a domino effect (Reniers and Cozzani, 2013). Therefore the modeling or assessment of the evolution of domino events is essential for protecting chemical and process installations against knock-on accidents. A growing public concern since the 1990s raised the attention in scientific and technical literature on domino effects (Necci et al., 2015).

Traditional risk identification and evaluation approaches such as HAZOP analysis, What–If analysis and the risk matrix are recommended for domino risk analysis in chemical industrial clusters (Reniers et al., 2005). Chemical industrial parks consist of various hazardous installations with different domino effect potentials. Some installations exhibit a high probability of initiating domino accidents while other installations are more likely to propagate domino events. These installations can be regarded as nodes, and the quantitative possibility of accident propagation may be represented by the weight of the links between nodes in a network graph (Reniers and Dullaert, 2007). Based on this concept, critical installations contributing to possible domino effects can be identified and this information may support the allocation of domino prevention resources (Reniers et al., 2008; Zhang and Chen, 2011). The methodology was extended for vulnerability analysis and protection decision making by using graph theory metrics (e.g. betweenness and closeness) (Khakzad et al., 2017; Khakzad and Reniers, 2015; Khakzad et al., 2016). These quick and reliable graph-based approaches are able to assess domino risks within an entire industrial area and identify the most critical units. They are however unable to capture temporal evolution characteristics.

A Quantitative Risk Assessment (QRA) framework was proposed for domino effects mainly including three steps: the identification of domino scenarios, a frequency analysis, and a consequence assessment (Cozzani et al., 2005). Only the first level propagation is considered in the framework due to the complexity of higher level propagations. The damage probability models used in the QRA methodology were extended and improved by considering different escalation vectors such as radiation, overpressure, and fragments (Gubinelli and Cozzani, 2009a, b; Jia et al., 2017; Landucci et al., 2012; Landucci et al., 2009). For example, a damage probability model for fire escalation assessment is established based on the results of finite element models (FEM) and experimental data (Landucci et al., 2009), as shown in Eq. (1).

$$Pr = a + b\ln(ttf) \tag{1}$$

The damage probability model is called “probit model” and the probit value is related to the “time to failure” (*ttf*) of installations, the estimation time required to start the emergency operations and the estimation time required to start the mitigation actions. The parameters of *a* and *b* are determined by considering the uncertainty of emergency response and the *ttf* in the first level propagation. Hence the “probit model” may be unreasonable for accurately estimating the damage probability of installations in second level or higher level propagations due to the delay of the “time to failure” compared with the first level propagation. In other words, using the model may result in over-estimation of the probability propagation in second or higher levels. Taking an extreme case as an example, if a primary fire was controlled by emergency actions (such as cooling with water, external firefighters arriving) before the second level propagation, the propagation probability of the second level would be zero.

In addition, a simulation approach was proposed based on a Monte Carlo method to model higher level propagations. The approach successfully models the spatial evolution of domino accidents but the shortcoming is obvious, i.e. it is time-consuming (Abdolhamidzadeh et al., 2010). An agent-based modeling approach considering installations’ states was proposed to analyze the higher-level propagations and temporal dependencies (Zhang et al., 2017). The Monte Carlo simulation method is also used to solve the model, and takes a high computation time, especially for realistic chemical clusters with a large number of installations. Other simulation work concentrates on emergency response assessment and optimization (Zhou and Reniers, 2016; Zhou et al., 2016). Besides, a Bayesian network methodology was proposed to model domino effect propagation (Khakzad, 2015; Khakzad et al., 2013). The methodology can model higher level propagations while it is difficult to apply it to chemical clusters with a large number of installations (Khakzad and Reniers, 2015).

In the light of these findings and considering the evolution of domino effect research, the present work is aimed at establishing a new methodology for modeling the spatial-temporal evolution of domino effects (STED) and overcoming the above shortcomings. The spatial propagation and the temporal propagation are integrated using a chain of graphs. First, we expound on spatial-temporal evolution characteristics of domino accidents triggered by fire in section 2. Next, the STED methodology procedures, the Domino Evolution Graph (DEG) model and the corresponding algorithm of Minimum Evolution Time (MET) are all elaborated and explained in section 3, following by a case study in section 4 and the related discussion in section 5. Finally, conclusions are drawn in section 6.

2. Fire-based domino evolution

2.1 Spatial propagation

Propagation is the main characteristic of domino accidents, linking a primary scenario with one or several higher level scenarios. Propagation patterns are divided into three categories according to spatial propagation features: simple propagation, multilevel domino chain, and multilevel propagation (Reniers and Cozzani, 2013). These propagation patterns are shown in Fig.1 and can be defined as follows:

- Simple propagation: a primary scenario triggering a secondary scenario (a "one-to-one" correspondence).
- Multilevel domino chain: a multilevel propagation, i.e., a primary scenario triggers a second accident scenario, and the second accident scenario triggers a third accident scenario, and so on.
- Multilevel propagation: a complex propagation including parallel effects and/or synergistic effects. In severe domino accidents, the propagation of the primary accident results in several secondary scenarios, and the secondary scenarios also trigger more than one higher order scenarios, which can be defined as parallel effects (Reniers and Cozzani, 2013). Alternatively, several scenarios of a lower level may trigger a higher level scenario, and synergistic effects may thus be present. As shown in Fig.1, installation 2.1 triggers installations of 3.1, 3.2 and 3.3, which may be regarded as a parallel effect, and the installation 3.1 triggered by installations 1 and 2.1 can be considered to be a synergistic effect.

The parallel effect reflects the escalation capability of installations and the synergistic effect is related to the damage probability caused by the escalation. Thus the parallel effect and the synergistic effect are essential for modeling the complex evolution of domino effects.

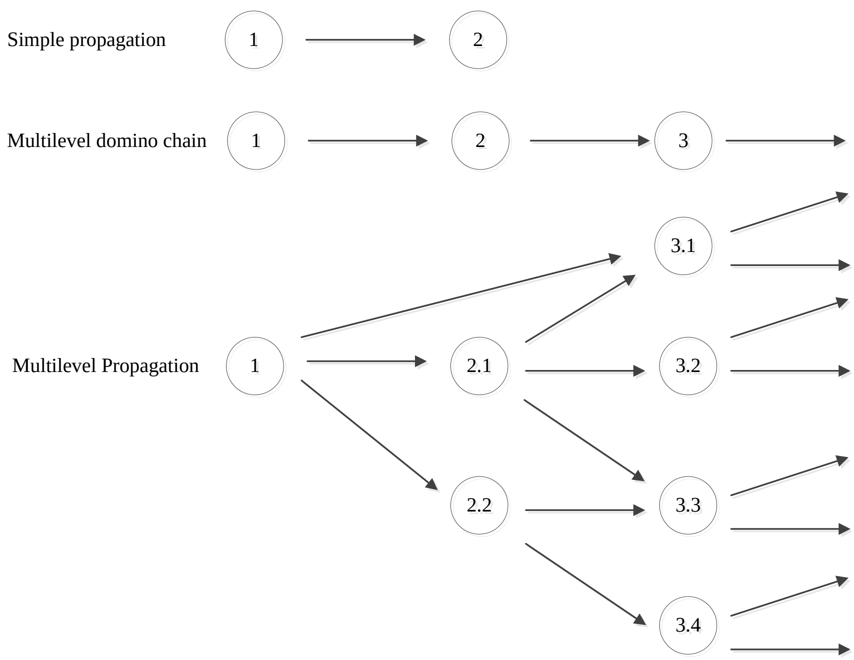

Fig. 1 Example of propagation patterns (Source: Reniers and Cozzani (2013)).

2.2 Temporal propagation

Fire scenarios such as pool fire and jet fire are responsible for most of the escalation events in industrial accidents (Gómez-Mares et al., 2008). These primary scenarios may induce serious heat loads on installations, possibly resulting in the failure of process units, storage vessels, pipework and other target installations by one or several of the following possible escalation vectors: heat radiation, fire engulfment, and fire impingement (Alileche et al., 2015; Landucci et al., 2009). Taking a simple propagation (a vessel to a vessel) as an example, the fire escalation process can be described as follows:

- The heat load is transferred from the fire to the target vessel by radiation and convection.
- The target vessel wall (shell) is heated and the temperature rises when radiation and convection are in progress.

- The heat transfers to the liquid and liquid vapor due to the existing temperature gradients among the vessel wall, the liquid and the liquid vapor in the vessel (conduction).
- The internal pressure of the vessel increases while the temperatures of the liquid and the liquid vapor rise.
- The above processes will continue until one of the following scenarios emerges: (1) vessel wall failure and loss of containment; (2) the fire is extinguished due to the burning out of the fuel; (3) the fire is controlled effectively by emergency response actions.

Higher-level propagations caused by fire occur when the target vessel fails, and in this case the escalation is delayed with respect to the start of the fire. The period of time between the start of the fire and the failure of the target equipment is called "time to failure" (*ttf*) (Necci et al., 2015). The escalation process can also end when the fuel burns out. The burning time of an installation is named "time to burn out" (*ttb*) (Khakzad et al., 2014). Similarly, the period of time between the start of the fire and the effective controlling of the fire is named "time to control effectively" (*ttc*) in this study.

As can be observed, the spatial propagation is an important characteristic in the evolution of domino effects triggered by fire. For integrating the spatial propagation and temporal propagation, a new methodology based on a chain of graphs for modeling the spatial-temporal evolution of domino effects (STED) is elaborated in the next section.

3. STED methodology

3.1 Overview

For modeling the spatial-temporal evolution of domino effects (STED) and obtaining the domino evolution graphs (paths), the evolution time and the evolution probability, a five-step methodology is proposed (Fig. 2).

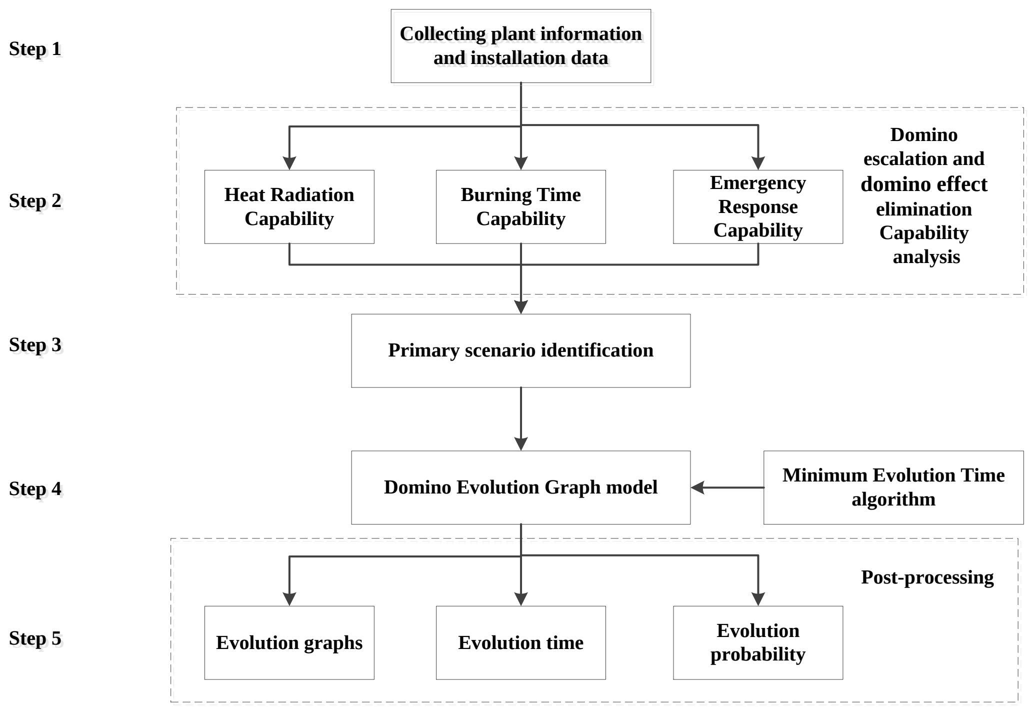

Fig. 2 Steps for performing STED methodology.

First, all necessary information of plants and installation data are collected, such as installation types, stored materials, process substances and emergency response plans. The second step analyzes the domino escalation capability of installations and the domino elimination capability of plants. Heat radiation and burning time data of installations is obtained, as well as the distribution function of *ttc*. Step 3 determines primary accident scenarios. The next step inputs all the above data into the Domino Evolution Graph (DEG) model and solves the model using the Minimum Evolution Time (MET) algorithm. Finally, step 5 conducts the post-processing of the results obtained in step 4 and thus delivers installations' damage probabilities and the corresponding advice on preventing domino accidents. The different steps will be elaborated hereafter.

3.2 Collecting plant information and installation data

Step 1 collects all necessary information and data for different steps of this methodology. The main plant information and installation data required to perform the STED methodology are summarized as follows:

- A layout of the chemical industrial park: installation positions, distances between different installations;
- installation data: installations' types, shapes, and sizes;
- Information of hazardous materials in installations: types, quantities, and states (e.g., phase state, pressure and temperature);
- Emergency response information: internal emergency response information and external emergency response information;
- Environmental parameters: temperature, wind direction, speed, humidity, etc.

The above information and data required are easy-to-collect and thus the step can be performed by either safety experts or plant employees.

3.3 Domino escalation and elimination capability analysis

3.3.1 Heat Radiation Capability (HRC)

The Heat Radiation Capability (HRC) of installations is an evaluation index of the domino escalation capability. It is obtained via heat radiation calculation in the second step of the methodology after collecting all the necessary information and data. Considering that n installations are identified in the first step, then the HRC matrix of dimension $n \times n$ can be obtained, as shown in Eq. 2. An element of HRC matrix (HRC_{ij}) denotes the heat radiation load caused by installation i on installation j if the installation i is on fire, in kw/m^2. The HRC_{ij} can, for instance, be obtained by the ALOHA software (Khakzad and Reniers, 2015a), or by other commercial software such as PHAST and FLUENT (Wang et al., 2013).

$$HRC = \begin{bmatrix} 0 & HRC_{12} & \cdots & HRC_{1n} \\ HRC_{21} & 0 & \cdots & HRC_{2n} \\ \vdots & & 0 & \vdots \\ HRC_{n1} & HRC_{n2} & \cdots & 0 \end{bmatrix} \tag{2}$$

$$HRC_{ij} \geq 0 \text{ if } i \neq j \tag{3}$$

$$HRC_{ij} = 0 \text{ if } i = j \tag{4}$$

3.3.2 Burning Time Capability (BTC)

The Burning Time Capability (BTC) of installations is another index required for evaluating the domino escalation capability. The Burning Time Capability matrix with dimension of $n \times 1$ consists of the *ttb* of all critical installations, as shown in Eq. (5) and Eq. (6). An element of BTC matrix (BTC_i) denotes the time to burn out (ttb_i) of installation i if i is on fire, in min. It can also be obtained by the ALOHA software (Khakzad, 2015). Both the HRC_{ij} and BTC_i can be seen as indexes for evaluating the domino escalation capability of installation *i*.

$$BTC = \begin{bmatrix} BTC_1 \\ BTC_2 \\ \vdots \\ BTC_n \end{bmatrix} \tag{5}$$

$$BTC_i = ttb_i \in R^+ \quad (i=1,2,3\cdots n) \tag{6}$$

3.3.3 Emergency Response Capability (ERC)

Emergency response plans in the chemical industry are essential to protect installations, the public, and workers' health and safety, to reduce the environmental impacts, and the recovery time of normal operations (Hosseinnia et al., 2018). The emergency response also influences the development of the accident and has important impacts on the occurring of domino effects (Zhou and Reniers, 2017). The emergency response time is affected by many human factors such as safety training and human response time, varying within different chemical plants. For performing static risk assessment, the uncertainty of the emergency response time is considered to obtain the "probit model" parameters (Landucci et al., 2009). In this study, the emergency response capability of a chemical plant is evaluated by the possible *ttc* values and the capability probability (*CP*). Considering there are *k* possible identified values of *ttc*, the Emergency Response Capability (ERC) matrix composed of *ttc* and *CP* can be represented by Eq. (7). The possible *ttc* values can be obtained by expert judgment, emergency exercises or other emergency simulation methods (Bandyopadhyay and Singh, 2016; Zhou and Reniers, 2017).

$$ERC = \begin{bmatrix} ttc_1 & CP_1 \\ ttc_2 & CP_2 \\ \vdots & \vdots \\ ttc_k & CP_k \end{bmatrix} \tag{7}$$

The ERC matrix presents a discrete distribution of *ttc* by providing limited *ttc* values and the cumulative probabilities. The discrete distribution can also be transformed into a continuous distribution by assuming a cumulative distribution function (ERC function) for the *ttc*. The parameters of the cumulative distribution function can be estimated by Maximum Likelihood Estimation (MLE) (Myung, 2003). For example, assuming a log-normal distribution (Landucci et al., 2009) of *ttc*, the distribution of *ttc* is denoted by Eq. (8)~ (10).

$$\log ttc \sim N\left(u, \sigma^2\right) \tag{8}$$

$$u = \frac{\sum_{i=1}^{k} \ln ttc_i}{k} \tag{9}$$

$$\sigma^2 = \frac{\sum_{i=1}^{k} \left(\ln ttc_i - u\right)^2}{k} \tag{10}$$

In Eq. (8), *u* is the mean of log *ttc* or expectation of the distribution; σ is the standard deviation of log *ttc* and σ^2 is the variance; ttc_i is the *i*th possible value of *ttc*. It should be noted that the cumulative distribution function should satisfy hypothesis testing. Therefore, the capability probability (*CP*) given any *ttf* value can be obtained by the ERC function, as shown in Eq. (11).

$$CP = \mathrm{ERC}(ttc) \tag{11}$$

3.4 Primary scenario identification

Possible primary scenarios are identified according to the plant information and installation data collected in step 1. The primary scenarios are divided into two categories: intentional scenarios and unintentional scenarios. Intentional scenarios can be obtained by any security risk assessment methodology, including threat analysis, vulnerability analysis and consequence analysis (API, 2013). Game theory approaches are widely used to analyze the intentional scenarios by considering strategies of defenders and adversaries (Reniers et al., 2015; Zhang and Reniers, 2016). Unintentional scenarios can be identified by traditional approaches such as HAZOP analysis, What-If analysis, and Fault-Tree analysis. Different from the previous domino risk assessment methodologies mainly identifying the scenario related to only one installation, the methodology proposed in this paper also accounts for the primary scenario involving multiple installations.

3.5 Modelling spatial-temporal evolution of domino accidents

3.5.1 State model

Installations in chemical plants are the main contributors to domino accidents. Four states of installations may be present in evolution processes according to a chronological sequence because domino accidents caused by heat radiation have distinct temporal characteristics. Table 1 describes the four states: “normal”, “heating up”, “fire” and “extinguished”. It should be emphasized that installations with a “normal” state, “heating up” state or “extinguished” state are regarded to exhibit no heat radiation on other installations. These states are named “no-escalation” states. Alternatively, “escalation” state defines a “fire” state causing heat radiation on target installations.

Table 1 State description.

State	Description
Normal	The installation operates normally in an initial state, and the state is assumed to be invariable without external interferences.
Heating up	The installation is not physically damaged but is heating up due to heat radiation received from installations with the “fire” state. This is a transition state: the state can transfer to either “normal” state or “fire” state.
Fire	The installation is on fire due to an unintentional primary scenario or due to escalation from an external installation. It is also a transition state and can only transfer to the “extinguished” state.
Extinguished	The installation fire is extinguished due to burning out of fuel or effective emergency response. This is a termination state.

There are four transfer relationships among these states, as shown in Fig. 3. “No-escalation” states are marked as an ellipse and the “escalation” state is marked as a circle in Fig. 3. All the states can only transfer to the next state except the state of “heating up” which possibly changes to a “normal” state or a “fire” state according to the heat radiation received. The transfer relationships related to the “fire” state are essential for domino evolution because these transfers change the heat radiation load of the system.

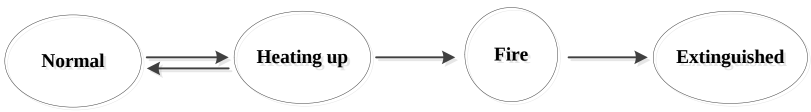

Fig. 3 State transfer relationships.

3.5.2 Domino evolution stage model

For modeling the spatial-temporal evolution of a domino accident, time is a distinct factor for evolution because time is related to the installations' damage and the performance of emergency response. The evolution time is dispersed into discrete time nodes by transfers related to the "fire" state. Each period between two adjacent time nodes is a stage. The evolution stage m counts the occurrence number of the "fire" state and the "extinguished" state from the beginning of the evolution to the present stage, as shown in Eq. (12). The time of evolution stage m (t_m) defines the period of time between two adjacent time nodes. So the t_m varies with different transfer types and different installations and it is determined in section 3.5.4.

$$m = \begin{cases} 0 & (\text{if all installations are in the "normal" state}) \\ m+1 & (m<M, \text{if an installation's state transfers to "fire" or "extinguished"}) \end{cases} \tag{12}$$

Where M is the total number of stages of a domino evolution process. For a domino evolution process, the influence of the current stage can be superimposed to the next stage (i.e., superimposed effects). According to the superimposed effects, a Domino Evolution Graph (DEG) model with a chain of graphs corresponding to the stages is proposed in the following section.

3.5.3 Domino Evolution Graph (DEG) model

A Domino Evolution Graph (DEG) is defined as a chain of graphs connected sequentially by superimposed effects, i.e., the next stage graph is only related to the graph of the current stage. Fig. 4 depicts a Domino Evolution Graph with 4 sequential graphs. The DEG_4 is determined by DEG_3, DEG_3 by DEG_2 and DEG_2 by DEG_1. The domino accident begins when installation 1 is on fire (a primary scenario) and ends when installation 3 catches fire caused by the escalation.

A domino graph in stage m of the DEG (DEG_m) consists of vertices (installations), directed edges (escalation vectors) and the related parameters. The domino graph in stage m can be presented as follows:

$$DEG_m = (N, S, E, EH, HR, RF, RB) \tag{13}$$

(1) N: is a set of vertices represent installations. The N doesn't change over time and can be expressed as the following:

$$N = \begin{bmatrix} 1 \\ 2 \\ \vdots \\ n \end{bmatrix} \tag{14}$$

(2) S: is a set of states denoting the state of installations in evolution stage m. The S can be expressed as follows:

$$S = \begin{bmatrix} S_1 \\ S_2 \\ \vdots \\ S_n \end{bmatrix} \tag{15}$$

In the Domino Evolution Graph, the states are represented by the vertices' colors: "white" represents "normal" state, "yellow" represents "heating up" state, "red" represents "fire" state and "gray" represents "extinguished" state.

(3) E: is a matrix with dimension of $n \times n$ representing a set of directed edges from installations with the "fire" state to installations with the "heating up" state in stage m. In this study, we set a threshold

(1kW/m^2) (Zhang et al., 2017) to judge whether there is a directed edge between each pair of installations. The two installations are connected by a directed edge when the heat radiation caused by installation *i* on installation *j* is greater than 1kW/m^2. An element of matrix *E* (E_{ij}) is determined by Eq. (16). The domino evolution will continue until there is no edge, i.e., *SE* =0. *SE* is the sum of all the elements of the matrix *E*, determined by Eq. (17). The row *i* of matrix *E* represents a parallel effect caused by installation *i*, and the column *j* of matrix *E* represents a synergistic effect received by installation *j*.

$$E_{ij}=\begin{cases}0 & \text{if there is no directed edge from installation } i \text{ to installation } j\\ 1 & \text{if there is a directed edge from installation } i \text{ to installation } j\end{cases} \tag{16}$$

$$SE=\sum_{i=1}^{n}\sum_{j=1}^{n}E_{ij} \tag{17}$$

(4) *EH*: is a matrix of dimension $n\times n$ denoting the directions and values of heat radiation in stage *m*. Any element of the matrix EH_{ij} is determined by the Heat Radiation Capability (HRC) matrix and *E*, as shown in Eq. (18).

$$EH_{ij}=HRC_{ij}\cdot E_{ij} \tag{18}$$

(5) *HR*: is a set of heat radiation loads received by installations in the evolution stage *m*. Considering the synergistic effects of spatial evolution, the heat radiation received by installation *j* is equal to the sum of heat radiation loads caused by other installations on installation *j*, as shown in Eq. (19).

$$HR_j=\sum_{i=1}^{n}EH_{ij}\quad\left(j=1, 2\cdots n\right) \tag{19}$$

(6) *RF*: is a set of residual time to failure of all installations in the evolution stage *m*. For the first evolution step (without superimposed effects), the *RF* can be estimated by the lumped model (Landucci et al., 2009), as shown in Eq. (20).

$$\log_{10}\left(RF_j^{\,1}\right)=c\log_{10}\left(HR_j^{\,1}\right)+d \tag{20}$$

Where *c* and *d* are constants given a special volume, *V* (m^3), as shown in Table 2. This lumped model is obtained by assuming that a failure occurred when the equivalent intensity of combined stress is greater than the maximum allowable stress (Landucci et al., 2009). The worst condition is considered in higher level propagations: the installation is on fire when it fails (Khakzad, 2015; Khakzad et al., 2013). The *HR* also varies over time in the spatial-temporal evolution because of superimposed effects. So the *RF* in higher level stages can't be directly determined by Eq. (20). For stage *m* (*m*>1), first calculate the *ttf* only under the radiation load in stage *m* (HR_j^{m}), namely,

$$\log_{10}\left(ttf_j^{\,m}\right)=c\log_{10}\left(HR_j^{\,m}\right)+d \tag{21}$$

With respect to the same installation or installations with the same volume, Eq. (21) can be rewritten as follows:

$$ttf_j^{\,m}=10^d\left(HR_j^{\,m}\right)^c \tag{22}$$

It is obvious that $ttf_j^{\,m}$ is directly proportional to $\left(HR_j^{\,m}\right)^c$ (*c*<0)， so a simple recurrence formula is obtained to estimate the *RF* as shown in Eq. (23):

$$RF_j^{\,m}=\left(\frac{HR_j^{\,m}}{HR_j^{\,m-1}}\right)^c\cdot\left(RF_j^{\,m-1}-t_{m-1}\right)\qquad(\mathrm{m}>1) \tag{23}$$

Integrating Eq. (21), Eq. (22) and Eq. (23), a general expression of *RF* in stage *m* is obtained:

$$RF_j^{\,m} = \begin{cases} 10^{d}\left(HR_j^{\,m}\right)^{c} & (m=1) \\ \left(\dfrac{HR_j^{\,m}}{HR_j^{\,m-1}}\right)^{c}\cdot\left(RF_j^{m-1}-t_{m-1}\right) & (m>1) \end{cases} \tag{24}$$

(7) *RB*: is a set of residual time to burn out of all installations in evolution stage *m*. If the state of installation *i* transfers from “heating up” to “fire” at the beginning of stage *m*, RB_i can be calculated as follows:

$$RB_i^{\,m} = BTC_i \tag{25}$$

$$RB_i^{\,m+1} = BTC_i - t_m \tag{26}$$

In other cases, the RB_i is regarded as infinite.

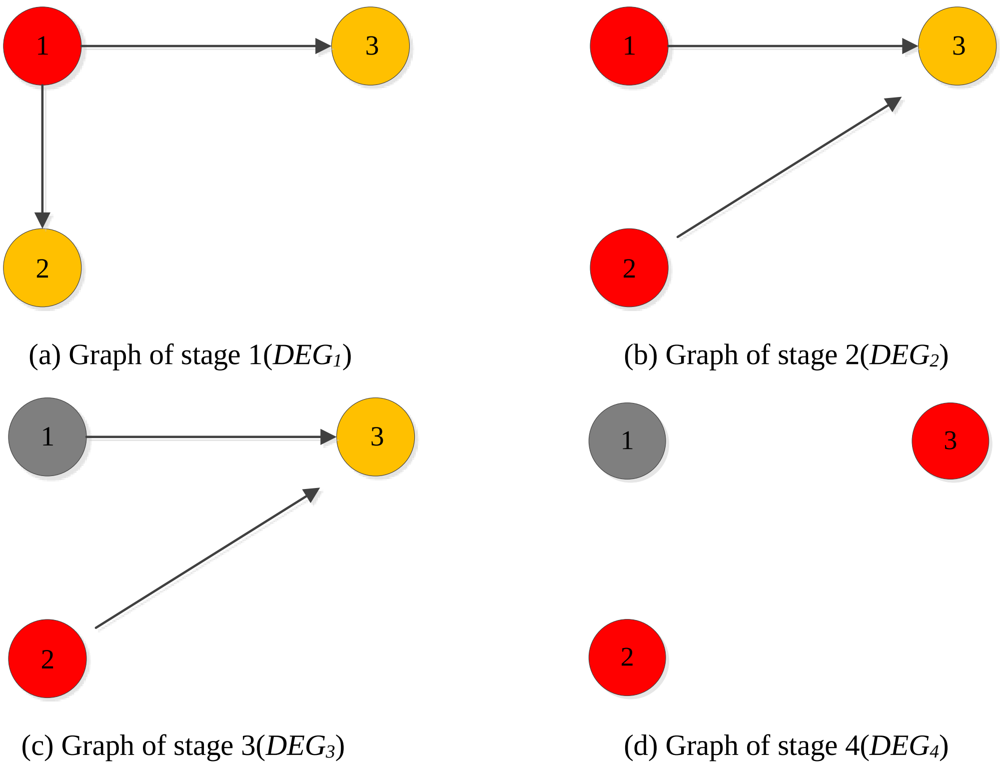

(a) Graph of stage 1(DEG_1)

(b) Graph of stage 2(DEG_2)

(c) Graph of stage 3(DEG_3)

(d) Graph of stage 4(DEG_4)

Fig.4 An example of a domino evolution process presented by the Domino Evolution Graph.

Table 2 The parameter value of *c* and *d*.

Installation	*c*	*d*
Atmospheric tank	-1.13	$-2.67\times10^{-5}\,V+9.9$
Pressurized tank	-0.95	$8.845V^{0.032}$

3.5.4 Evolution principle

In stage *m* of the evolution, the next stage (*m*+1) is determined by the minimum time of *RF* and *RB*, namely,

$$t_m = \min(RB_i, RF_j)\ i, j = 1, 2, \cdots n \tag{27}$$

Thus the total evolution time at the beginning of stage m (T_m) can be obtained by Eq. (28).

$$T_m = \begin{cases} 0 & (m = 1) \\ T_{m-1} + t_{m-1} & (m > 1) \end{cases} \tag{28}$$

Finally, the probability of stage m (P_m) is calculated by using the distribution function of ERC, as shown in Eq. (29).

$$P_m = 1 - \mathrm{ERC}(T_m) \tag{29}$$

The evolution principle indicates that an evolution enters into the next stage when any installation's state transfers to 'fire' or 'extinguished'. And the evolution ends when SE=0 or $P_m < P_{min}$ (P_{min} is the minimum probability settled by experts).

3.5.5 Minimum Evolution Time (MET) algorithm

In this section, the Minimum Evolution Time (MET) algorithm is proposed to solve the Domino Evolution Graph model. Fig. 5 shows the flowchart of the MET algorithm.

The MET algorithm flowchart can be explained as follows. First, all installations are in the "normal" state and all basic data are inputted in stage 0. Next, model parameters including S, E, and EH are updated according to the primary scenario. If there are installations with the "heating up" state, then the evolution will continue, otherwise, the evolution will be terminated. Third, the *HR is* calculated according to Eq. (19). The *RF* in stage *m* is updated based on the current *HR*, the *HR* and *RF* in the last stage (*m*-1) using Eq. (24). Similarly, the *RB* in stage *m* is updated based on the time of the last stage T_{m-1} and the *RB* in the last stage (*m*-1) using Eq. (25) and Eq. (26). Afterwards, the time of the current stage can be obtained according to the principle of minimum evolution time. Finally, the probability of the next stage P_{m+1} is obtained by using Eq. (29). The evolution will enter into the next stage (*m*+1) and the above steps will continue until the probability P_{m+1} is less than a minimum value P_{min}.

Using this algorithm, the stage time, the graph of each stage, and the probability of each stage can be obtained quickly. It is obvious that the algorithm has a fast convergence speed because of the maximum evolution stage less than 2*n* (i.e, all installations are damaged). The number of iterations is linearly related to the number of installations, which is a huge advantage for the methodology's application in practical chemical industrial parks with possibly hundreds or even thousands of installations and installation parts to be taken into account for the domino effect assessment.

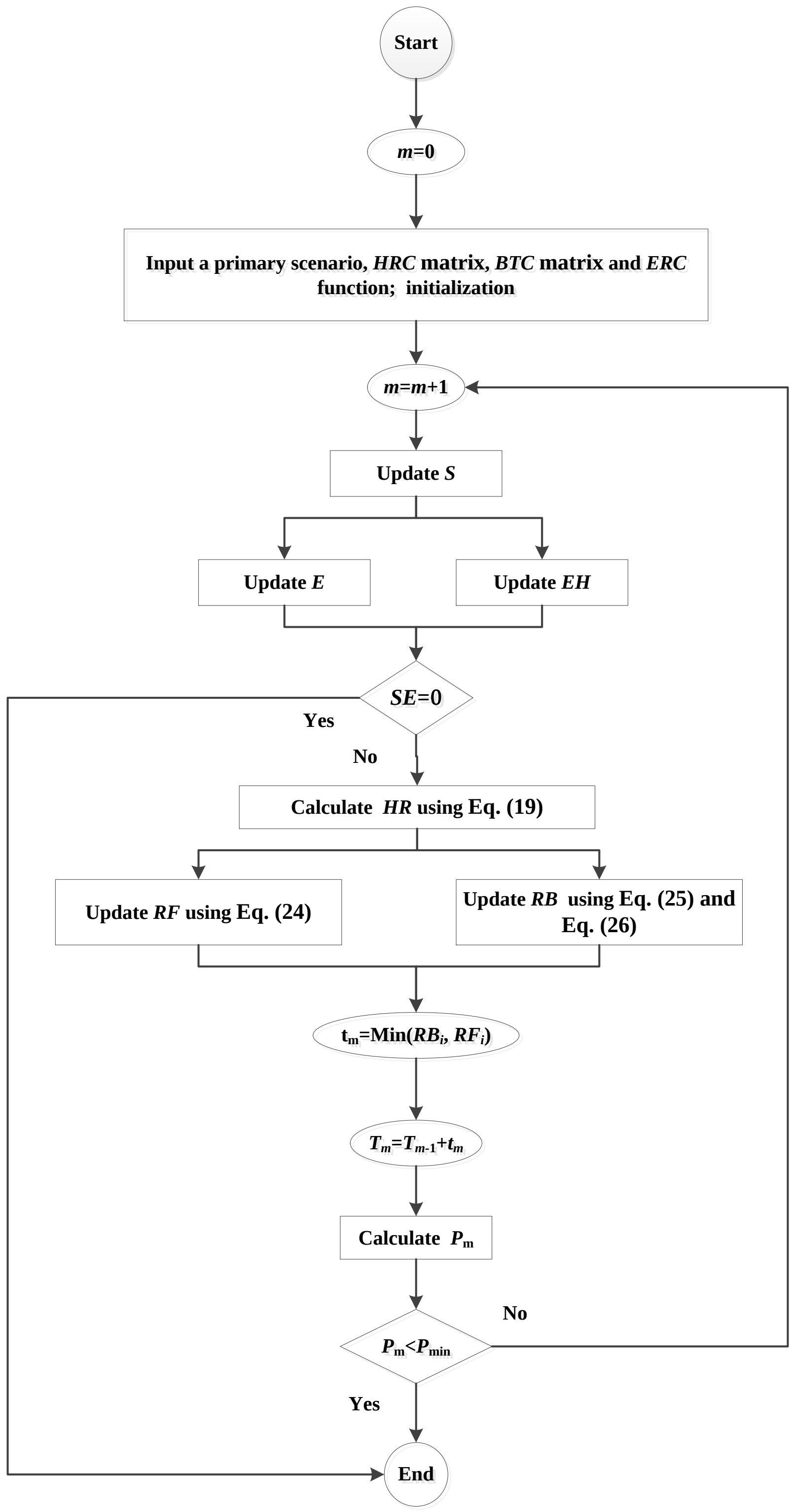

Fig. 5 Flowchart of the Minimum Evolution Time (MET) algorithm.

3.6 Post-processing

The domino evolution graphs, the evolution time, and the evolution probability of a primary scenario are obtained by using the DEG model and the MET algorithm in step 4. The objective of post-processing is to analyze the results to obtain the damage probability of installations and evaluate the escalation capability of the primary scenario. The installation's damage probability is equal to the stage probability if the installation fails in the stage while it is zero if the installation is not damaged in the entire evolution process. The escalation capability of the primary scenario is evaluated by the number of installations possibly damaged and the damage probability. Finally, the step also provides advice on safety and security resource allocation for preventing domino accidents based on the damage probability analysis and the escalation capability analysis.

4. Illustrative case study

For illustrative purposes, the fundamentals of the methodology are demonstrated via an illustrative tank storage area. The layout of the area is shown in Fig. 6. The features of the tanks are summarized in Table 3. Considering the primary accident probability of each tank caused by safety events is 10^{-5}. Assuming a log-normal distribution of the time to control effectively (*ttc*), i.e., $\log ttc \sim \left(\mu,\sigma^2\right)$, the mean of *ttc* is equal to 10 min and the corresponding variance is equal to 2 min.

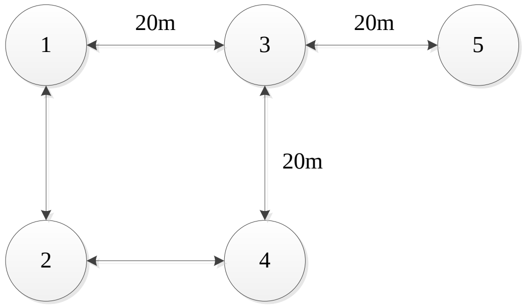

Fig. 6 Scheme of an illustrative chemical plant with five atmospheric storage tanks.

Table 3 Features of chemical storage tanks in the plant.

Tank	Type	Dimension (m^3)	Chemical substance	Size (m^3)	Chemical content (t)
1	Atmospheric	10×6.5	Benzene	500	350
2	Atmospheric	7.0×5.5	Benzene	200	120
3	Atmospheric	10×6.5	Acetone	500	300
4	Atmospheric	7.0×5.5	Acetone	200	140
5	Atmospheric	7.0×5.5	Acetone	200	15

Let us assume that the main environmental parameters are as follows: a wind speed of 1m/s measured at 10m above the ground and blowing from Northwest, partly cloudy, air temperature of 25℃, 50% relative humidity, and stability class of E. The heat radiation caused by pool fire and the burning rate of each tank are calculated through the ALOHA software. The possible heat radiation load caused by tank *i* on tank *j* (i.e., HRC_{ij}) is depicted in Table 4. Table 5 shows the burning rate and the *BTC* of all tanks.

Table 4 Heat Radiation Capability, *HRC* (kW/m^2).

	Tank *j*				
Tank *i*	1	2	3	4	5
1	-	20.3	20.3	12.3	6.7
2	20.3	-	12.3	20.3	5.4
3	15.6	9.0	-	15.6	15.6
4	9.0	15.6	15.6	-	9.0
5	4.68	3.76	15.6	9.0	-

Table 5 Burning Time Capability, *BTC*.

Tank *i*	Burn rate (kg/min)	BTC_i (min)
1	860	407.0
2	860	139.5
3	817	367.2
4	817	171.4
5	817	18.4

Three unintentional primary scenarios are assumed as follows: (1) a pool fire on tank 1; (2) a pool fire on tank 5; (3) simultaneous pool fires on tank 1 and 5. Using the STED methodology proposed in this paper, three DEGs corresponding to the three primary scenarios are obtained and separately shown in Fig. 7, Fig. 8 and Fig. 9.

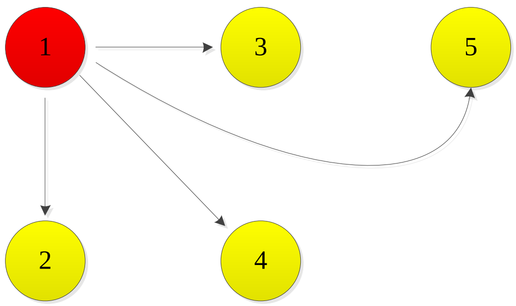

(a) Graph of stage 1 at T=0 min

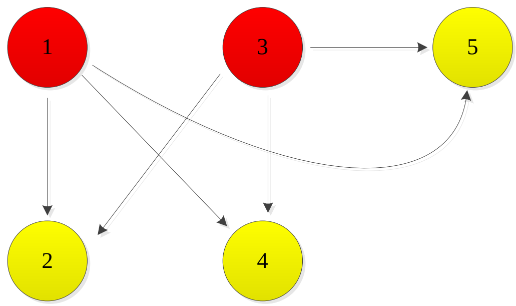

(b) Graph of stage 2 at T=10.9 min

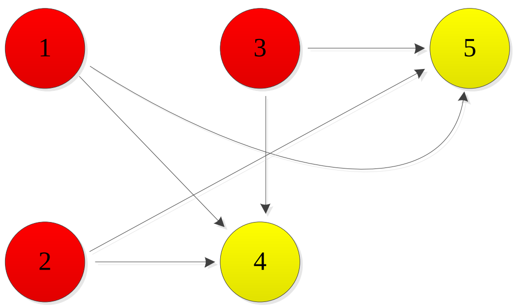

(c) Graph of stage 3 at T=11.0 min

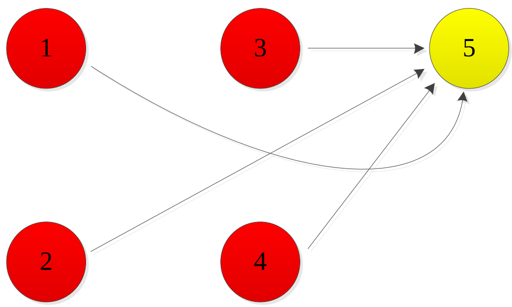

(d) Graph of stage 4 at T=12.8 min

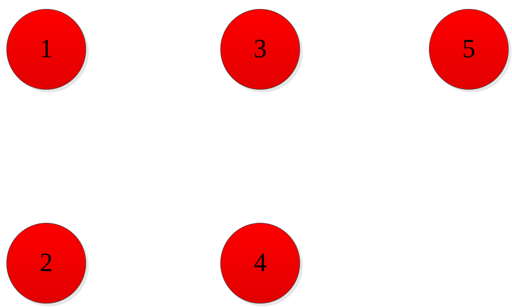

(e) Graph of stage 5 at T=15.5 min

Fig. 7 Domino Evolution Graph of primary scenario (1): a pool fire on tank 1.

Fig. 7 depicts the evolution process of primary scenario (1). In the first stage, tank 1 is on fire, the heat radiation produced by tank 1 is received by tank 2, 3, 4 and 5. Stage 2 starts at T=10.9 min when tank 3 is on fire, following by tank 2 in stage 3, inducing synergistic effects on other tanks and accelerating the evolution. In stage 4, tank 4 catches fire at T=12.8 min. Finally, the evolution ends in stage 5 when all the tanks are on fire.

The evolution process of the second scenario is shown in Fig. 8. For the scenario, tank 5 burns out at stage 3 after tank 3 catches fire, so the evolution is slower than the evolution of the first scenario. The evolution ends when tank 2 is on fire. So all tanks may be damaged under this primary scenario.

The methodology proposed in the study can model different kinds of primary scenarios, even including the scenario involving multiple installations, as shown in Fig. 9. In this case, both tank 1 and tank 5 are on fire simultaneously in the first stage. A synergistic effect caused by tank 1 and tank 5 results in the rapid failure of tank 3 at T=5.7min. The domino accident propagates rapidly and terminates at T=8.1min due to the combination of synergistic effects and superimposed effects.

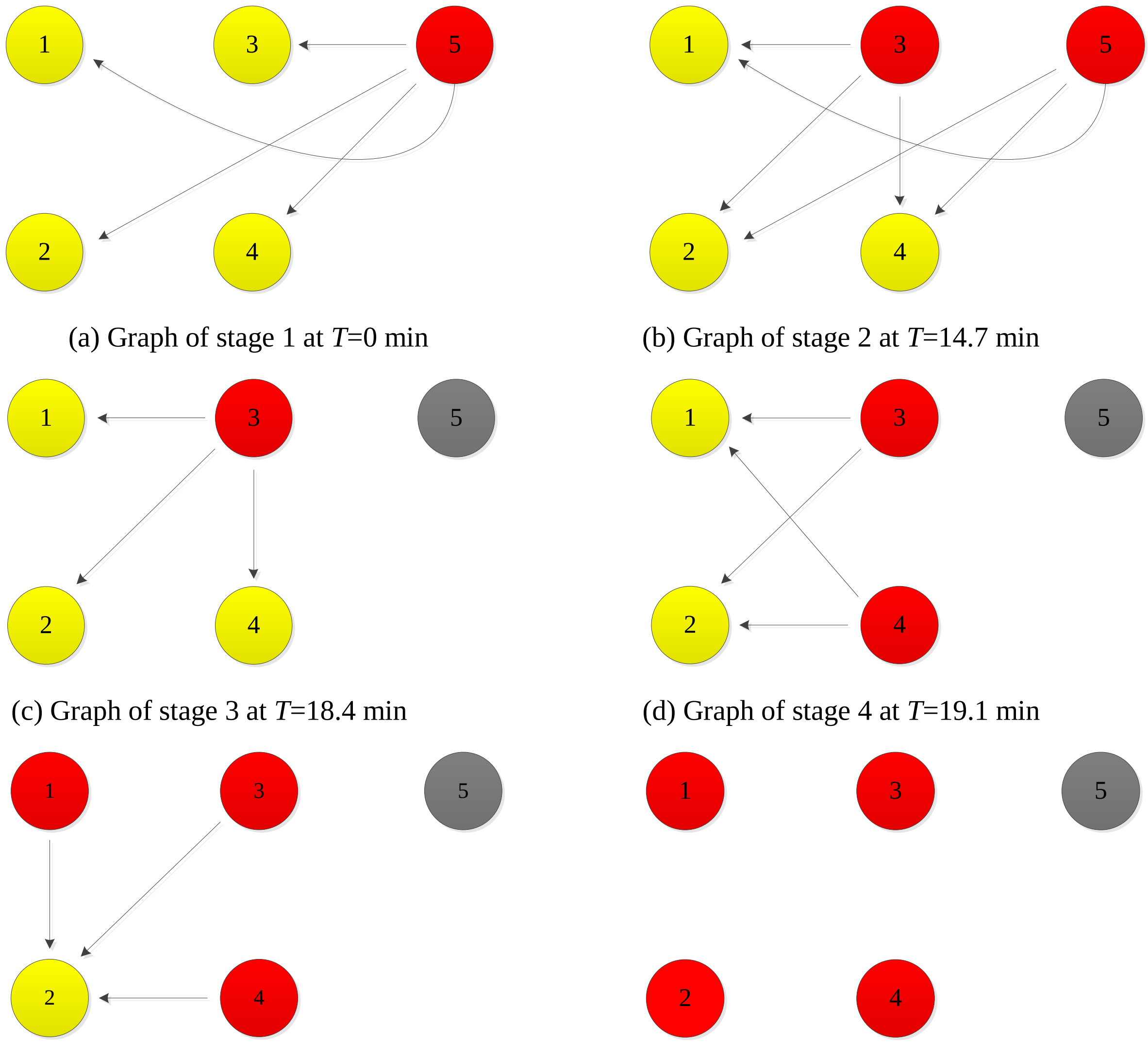

(a) Graph of stage 1 at T=0 min (b) Graph of stage 2 at T=14.7 min
(c) Graph of stage 3 at T=18.4 min (d) Graph of stage 4 at T=19.1 min
(e) Graph of stage 5 at T=22.2 min (f) Graph of stage 6 at T=23.3 min

Fig. 8 Domino Evolution Graph of primary scenario (2): a pool fire on tank 5.

The probability of each evolution stage with different primary scenarios is shown in Table 6. It is obvious that the probability of each stage in the primary scenario (1) is higher than that in the primary scenario (3) because the former evolution speed is lower than the latter. In other words, the likelihood of the domino effect being eliminated by emergency response actions increases with decreasing the evolution speed. The probability of each stage in the primary scenario (3) is in the same order of magnitude due to the highest evolution speed. The results are coincident with reality since the probability of *ttc* increases over time. The damage probability of each tank can be obtained, as shown in Table 7. The damage probability of each tank in the first scenario is higher than that in the second scenario, which indicates that the occurrence probability of a domino accident increases with increasing heat radiation caused by the primary scenario. The difference of the probability among each tank is very small in scenario (3), demonstrating that the escalation range increases with a growing number of primary events. The damage probability of tank 3 is the highest in all of the cases because tank 3 is the first to be damaged, that is, tank 3 is more likely to be damaged by domino propagation and should be allocated more safety barriers. Compared with tank 5, tank 1 has a higher probability of initiating domino effects and is more likely to be attacked by terrorists. Thereby more security resources should be allocated to tank 5. The probability of the third primary scenario with two tanks on fire simultaneously (10^{-10}) is lower than the first primary scenario (10^{-5}) and the second primary scenario (10^{-5}). The primary scenario similar to scenario (3) is more likely to occur when the area is attacked by terrorists. So primary scenarios related to multiple installations cannot be ignored compared with primary scenarios where only one installation is damaged, since domino effects may be inevitable once the scenario occurs (as shown in table 5).

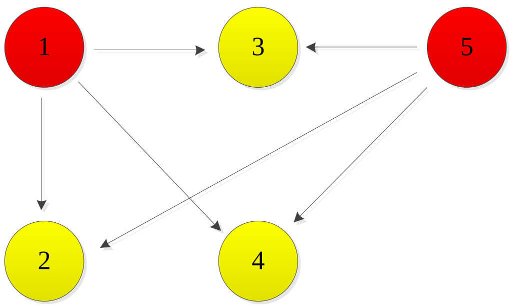

(a) Graph of stage 1 at T=0 min

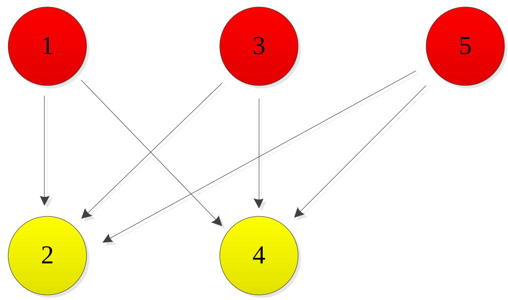

(b) Graph of stage 2 at T=5.7 min

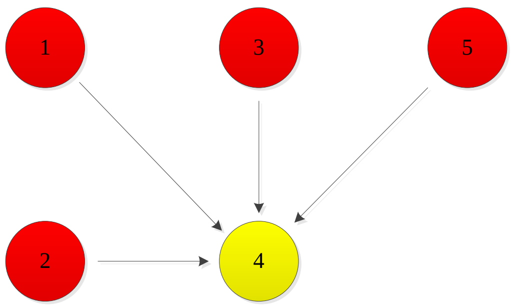

(c) Graph of stage 3 at T=8.0 min

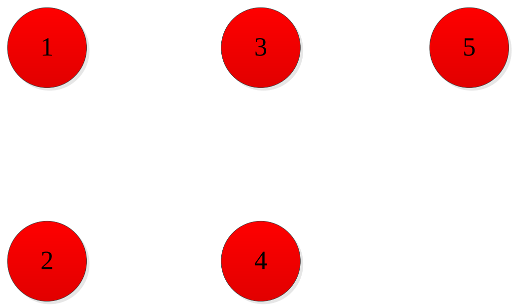

(d) Graph of stage 4 at T=8.1 min

Fig. 9 Domino Evolution Graph of primary scenario (3): pool fires on tank1 and tank 5.

Table 6 Domino evolution stages and the corresponding probability.

Primary scenario	Stage 1	Stage 2	Stage 3	Stage 4	Stage 5	Stage 6
1	10^{-5}	0.24×10^{-5}	0.23×10^{-5}	0.36×10^{-6}	0.77×10^{-7}	-
2	10^{-5}	0.25×10^{-7}	0.53×10^{-10}	0.14×10^{-10}	0.43×10^{-13}	0.65×10^{-14}
3	10^{-10}	1.00×10^{-10}	0.93×10^{-10}	0.91×10^{-10}	-	-

Table 7 Damage probability of each tank in different unintentional primary scenarios.

Primary scenario	Tank 1	Tank 2	Tank 3	Tank 4	Tank 5
1	1.00×10^{-5}	0.23×10^{-5}	0.24×10^{-5}	0.36×10^{-6}	0.77×10^{-7}
2	0.43×10^{-13}	0.65×10^{-14}	0.25×10^{-7}	0.14×10^{-10}	1.00×10^{-5}
3	1.00×10^{-10}	0.93×10^{-10}	1.00×10^{-10}	0.91×10^{-10}	1.00×10^{-5}

5. Discussion

The case study implemented in section 4 demonstrates that the STED methodology is an effective tool to model the domino evolution process triggered by fire. The domino evolution graphs (paths), domino evolution time, and the evolution probability can be obtained by using the DEG model and the MET algorithm proposed in this methodology. The methodology can also model different kinds of primary scenarios and capture the characteristic that the damage probability of installations decreases with increasing the evolution time due to emergency response.

Table 8 shows the residual time to failure (*RF*) of each tank in the evolution process of scenario (1). The obvious acceleration of evolution demonstrates that superimposed effects and synergistic effects play important roles in the evolution process. For example, tank 3 catches fire at T=10.9 min and tank 2 catches fire at T=11.0 min. The time of stage 2 (t_2) is only 0.1 min but the residual time to failure of tank 4 (RF_4) is shorted by 1.6 min due to the synergistic effect in stage 3 caused by tank 1 and tank 2.

Table 8 Residual time to failure (*RF*) of each tank in scenario (1)

Tank	Residual time to failure (*RF*) in different stages (min)				
	Stage 1	Stage 2	Stage 3	Stage 4	Stage 5
1	-	-	-	-	-
2	11.0	0.1	-	-	-
3	10.9	-	-	-	-
4	19.4	3.4	1.8	-	-
5	38.5	7.1	5.5	2.7	-

Fig. 10 illustrates curves of evolution time T versus evolution stages of primary scenario (1) under the condition (i) with superimposed effects and (ii) regardless of superimposed effects by using a heat radiation threshold (15 kW/m^2). The former is represented by a dotted curve and the latter is marked by a solid curve. The evolution sequence doesn't change but the time nodes of stage 4 and 5 are respectively delayed by 2.3 min and 2.6 min, regardless of superimposed effects. Therefore, the severity of domino effects is underestimated, regardless of either superimposed effects or synergistic effects, which may cause huge losses.

Fig. 11 depicts the evolution graphs of scenario (2) regardless of the Burning Time Capability of tanks. The evolution stage, evolution sequence and evolution time are totally different from the evolution process considering the Burning Time Capability (as shown in Fig. 8). The emergency resources may be allocated unreasonably if the Burning Time Capability is not considered. For instance, excessive emergency resources may be assigned to tank 5 thus weakening the elimination capability of domino effects.

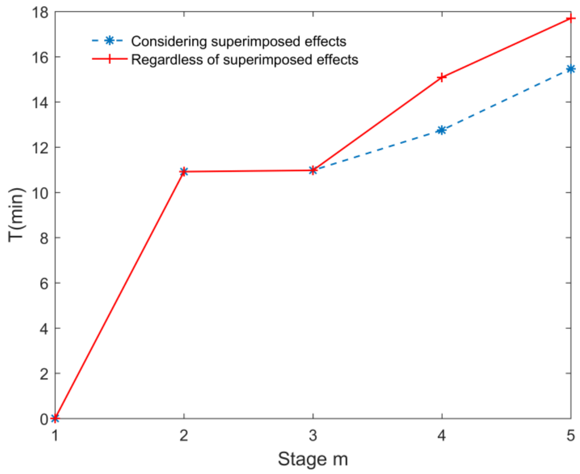

Fig. 10 Curves of evolution time *T* versus evolution stage *m*.

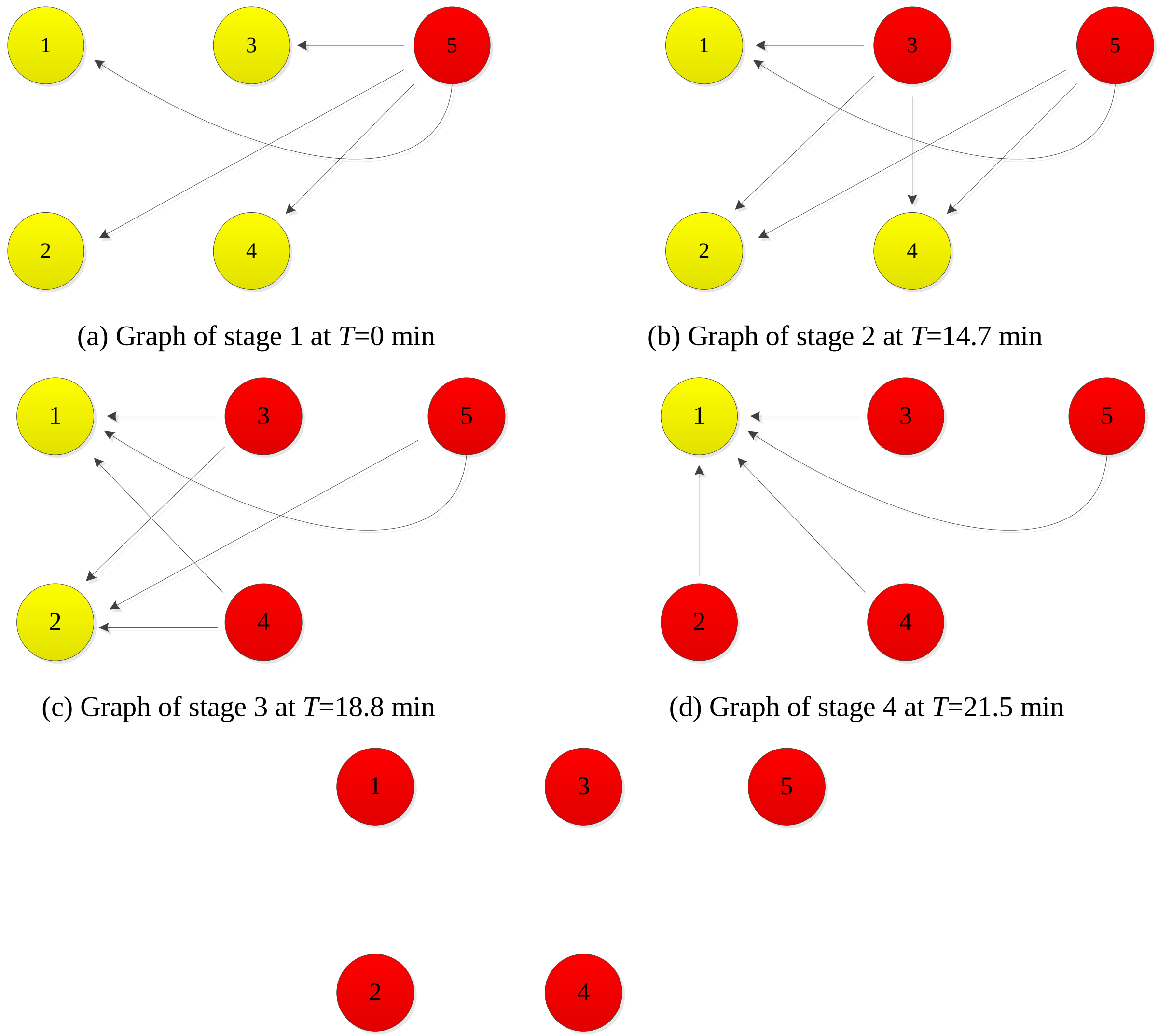

(a) Graph of stage 1 at *T*=0 min

(b) Graph of stage 2 at *T*=14.7 min

(c) Graph of stage 3 at *T*=18.8 min

(d) Graph of stage 4 at *T*=21.5 min

(e) Graph of stage 5 at *T*=22.4 min

Fig. 11 Domino Evolution Graph of primary scenario (3) regardless of *BTC*.

In this study, the DEG model can easily be solved by the Minimum Evolution Time (MET) algorithm, avoiding the time-consuming approach of repeatedly generating random numbers. The maximum number of iterations of the MET algorithm is 2*n* while the minimum number of iterations of Monte Carlo-based simulation tools is 10^6 (Abdolhamidzadeh et al., 2010; Zhang et al., 2017). So the calculation efficiency is improved greatly. For the case with 5 installations, the maximum number of iterations is 10. The real iteration in scenario (1) is 5, 6 in scenario (2) and 4 in scenario (3). The calculation time is dramatically shorted (e.g., the scenario (1) with 5 iterations only takes 0.018s). Thus this methodology can truly be applied to real-life chemical industrial parks containing hundreds or thousands of chemical installations. For example, for a real chemical cluster with 227 installations (Reniers et al., 2008), the maximum number of iterations of an evolution is only 454. So this methodology can be applied to predict the potential attack targets in large chemical parks. Besides, further research may focus on modeling the uncertainty of ignition after installations' failure and considering the effects of safety barriers on the accident evolution.

6. Conclusions

In this study, a methodology including a Domino Evolution Graph (DEG) model and a Minimum Evolution Time (MET) algorithm is proposed to model the evolution of domino accidents. The evolution process is divided into stages according to chronological order. Each stage starts with the occurrence of a "fire" state or an "extinguished" state and also ends with a new 'fire' state or an 'extinguished' state emerging. The characteristics of each evolution stage are modeled by a graph consisting of vertices (installations), directed edges (escalation vectors) and the related parameters. All the graphs of a domino evolution process are sequentially connected by superimposed effects, making up a Domino Evolution Graph. The Minimum Evolution Time (MET) algorithm based on the principle of minimum evolution time is proposed to solve the DEG model. The model results, including evolution graphs, evolution time, and the evolution probability, can be quickly obtained by using this algorithm since the maximum number of iterations of the MET algorithm is 2*n*.

A case study shows that the proposed methodology is able to not only capture the spatial-temporal dimension but also overcome the limitation of the "probit model" approach in higher level propagations. The evolution graphs (paths), the evolution time and the damage probability of installations in second or higher level propagations can easily be obtained by this dynamic methodology. Besides, a quantitative analysis indicates that the synergistic effects, the superimposed effects and the installation's burning capability considered in the methodology have important effects on domino evolution and cannot be ignored. The primary scenario related to multiple installations cannot be ignored compared with primary scenarios where only one installation is on fire, because domino effects may be inevitable once the primary scenario occurs.

This study is the first work to employ a Domino Evolution Graph (DEG) approach modeling the spatial-temporal evolution of domino effects. The outcome of this research can be used to support the decision-making of safety and security barriers and emergency resources. Furthermore, this methodology can also be extended to domino risk (safety and security) assessment of an entire industrial park consisting of hundreds or even thousands of installations.

References

Abdolhamidzadeh, B., Abbasi, T., Rashtchian, D., Abbasi, S.A., 2010. A new method for assessing domino effect in chemical process industry. J Hazard Mater 182, 416-426.
Alileche, N., Cozzani, V., Reniers, G., Estel, L., 2015. Thresholds for domino effects and safety distances in the process industry: A review of approaches and regulations. Reliability Engineering & System Safety 143, 74-84.

API, 2013. ANSI/API Standard 780 – Security risk assessment methodology for the petroleum and petrochemical industry. American Petroleum Institute.
Bandyopadhyay, M., Singh, V., 2016. Development of agent based model for predicting emergency response time. Perspectives in Science 8, 138-141.
Cozzani, V., Gubinelli, G., Antonioni, G., Spadoni, G., Zanelli, S., 2005. The assessment of risk caused by domino effect in quantitative area risk analysis. J Hazard Mater 127, 14-30.
Gómez-Mares, M., Zárate, L., Casal, J., 2008. Jet fires and the domino effect. Fire Safety Journal 43, 583-588.
Gubinelli, G., Cozzani, V., 2009a. Assessment of missile hazards: evaluation of the fragment number and drag factors. J Hazard Mater 161, 439-449.
Gubinelli, G., Cozzani, V., 2009b. Assessment of missile hazards: identification of reference fragmentation patterns. J Hazard Mater 163, 1008-1018.
Hessami, A.G., 2004. A systems framework for safety and security: the holistic paradigm. Systems Engineering 7, 99-112.
Hosseinnia, B., Khakzad, N., Reniers, G., 2018. Multi-plant emergency response for tackling major accidents in chemical industrial areas. Safety Science 102, 275-289.
Jia, M., Chen, G., Reniers, G., 2017. An innovative framework for determining the damage probability of equipment exposed to fire. Fire Safety Journal 92, 177-187.
Khakzad, N., 2015. Application of dynamic Bayesian network to risk analysis of domino effects in chemical infrastructures. Reliability Engineering & System Safety 138, 263-272.
Khakzad, N., Khan, F., Amyotte, P., Cozzani, V., 2013. Domino effect analysis using Bayesian networks. Risk Anal 33, 292-306.
Khakzad, N., Khan, F., Amyotte, P., Cozzani, V., 2014. Risk management of domino effects considering dynamic consequence analysis. Risk Anal 34, 1128-1138.
Khakzad, N., Landucci, G., Reniers, G., 2017. Application of Graph Theory to Cost-Effective Fire Protection of Chemical Plants During Domino Effects. Risk Anal 37, 1652-1667.
Khakzad, N., Reniers, G., 2015. Using graph theory to analyze the vulnerability of process plants in the context of cascading effects. Reliability Engineering & System Safety 143, 63-73.
Khakzad, N., Reniers, G., Abbassi, R., Khan, F., 2016. Vulnerability analysis of process plants subject to domino effects. Reliability Engineering & System Safety 154, 127-136.
Landucci, G., Antonioni, G., Tugnoli, A., Cozzani, V., 2012. Probabilistic Assessment of Domino Effect Triggered by Fire: Implementation in Quantitative Risk Assessment. Chemical Engineering Transactions 26, 195-200.
Landucci, G., Gubinelli, G., Antonioni, G., Cozzani, V., 2009. The assessment of the damage probability of storage tanks in domino events triggered by fire. Accid Anal Prev 41, 1206-1215.
Myung, I.J., 2003. Tutorial on maximum likelihood estimation. Journal of mathematical Psychology 47, 90-100.
Necci, A., Cozzani, V., Spadoni, G., Khan, F., 2015. Assessment of domino effect: State of the art and research Needs. Reliability Engineering & System Safety 143, 3-18.
Reniers, G., Cozzani, V., 2013. Domino Effects in the Process Industries, Modeling, Prevention and Managing. Elsevier, Amsterdam, The Netherlands.
Reniers, G., Dullaert, W., Audenaert, A., Ale, B.J., Soudan, K., 2008. Managing domino effect-related security of industrial areas. Journal of Loss Prevention in the Process Industries 21, 336-343.
Reniers, G., Pavlova, Y., 2013. Using game theory to improve safety within chemical industrial parks. Springer.
Reniers, G., Van Lerberghe, P., Van Gulijk, C., 2015. Security risk assessment and protection in the chemical and process industry. Process Safety Progress 34, 72-83.
Reniers, G.L.L., Dullaert, W., 2007. DomPrevPlanning©: User-friendly software for planning domino effects prevention. Safety Science 45, 1060-1081.
Reniers, G.L.L., Dullaert, W., Ale, B.J.M., Soudan, K., 2005. Developing an external domino accident prevention framework: Hazwim. Journal of Loss Prevention in the Process Industries 18, 127-138.
Zhang, L., Landucci, G., Reniers, G., Khakzad, N., Zhou, J., 2017. DAMS: A Model to Assess Domino Effects by Using Agent-Based Modeling and Simulation. Risk Anal.
Zhang, L., Reniers, G., 2016. A Game-Theoretical Model to Improve Process Plant Protection from Terrorist Attacks. Risk Anal 36, 2285-2297.

Zhang, X., Chen, G., 2011. Modeling and algorithm of domino effect in chemical industrial parks using discrete isolated island method. Safety Science 49, 463-467.
Zhou, J., Reniers, G., 2016. Petri-net based simulation analysis for emergency response to multiple simultaneous large-scale fires. Journal of Loss Prevention in the Process Industries 40, 554-562.
Zhou, J., Reniers, G., 2017. Analysis of emergency response actions for preventing fire-induced domino effects based on an approach of reversed fuzzy Petri-net. Journal of Loss Prevention in the Process Industries 47, 169-173.
Zhou, J., Reniers, G., Khakzad, N., 2016. Application of event sequence diagram to evaluate emergency response actions during fire-induced domino effects. Reliability Engineering & System Safety 150, 202-209.